International Journal of Computer Assisted Radiology and Surgery
https://doi.org/10.1007/s11548-020-02229-5

ORIGINAL ARTICLE

A visual odometry base-tracking system for intraoperative C-arm guidance

Luke Haliburton[1] · Hooman Esfandiari[2] · Pierre Guy[3] · Carolyn Anglin[4,5,6] · Antony Hodgson[1]

Received: 13 February 2020 / Accepted: 6 July 2020

Abstract

Purpose C-arms are portable X-ray devices used to generate radiographic images in orthopedic surgical procedures. Evidence suggests that scouting images, which are used to aid in C-arm positioning, result in increased operation time and excess radiation exposure. C-arms are also primarily used qualitatively to view images, with limited quantitative functionality. Various techniques have been proposed to improve positioning, reduce radiation exposure, and provide quantitative measuring tools, all of which require accurate C-arm position tracking. While external stereo camera systems can be used for this purpose, they are typically considered too obtrusive. This paper therefore presents the development and verification of a low-profile, real-time C-arm base-tracking system using computer vision techniques.

Methods The proposed tracking system, called OPTIX (On-board Position Tracking for Intraoperative X-rays), uses a single downward-facing camera mounted to the base of a C-arm. Relative motion tracking and absolute position recovery algorithms were implemented to track motion using the visual texture in operating room floors. The accuracy of the system was evaluated in a simulated operating room mounted on a real C-arm.

Results The relative tracking algorithm measured relative translation position changes with errors of less than 0.75% of the total distance travelled, and orientation with errors below 5% of the cumulative rotation. With an error-correction step incorporated, OPTIX achieved C-arm repositioning with translation errors of less than 1.10 ± 0.07 mm and rotation errors of less than $0.17 \pm 0.02°$. A display based on the OPTIX measurements enabled consistent C-arm repositioning within 5 mm of a previously stored reference position.

Conclusion The system achieved clinically relevant accuracies and could result in a reduced need for scout images when re-acquiring a previous position. We believe that, if implemented in an operating room, OPTIX has the potential to reduce both operating time and harmful radiation exposure to patients and surgical staff.

Keywords C-arm · Computer vision · Tracked C-arm · Radiation · Orthopedic · Position tracking

✉ Luke Haliburton
luke.haliburton@ifi.lmu.de

1 Department of Mechanical Engineering, University of British Columbia, Vancouver, BC, Canada

2 Surgical Technologies Laboratory, Biomedical Engineering, University of British Columbia, Vancouver, BC, Canada

3 Department of Orthopaedics, University of British Columbia, Vancouver, BC, Canada

4 Department of Civil Engineering, University of Calgary, Calgary, AB, Canada

5 Biomedical Engineering, University of Calgary, Calgary, AB, Canada

6 McCaig Institute for Bone and Joint Health, Calgary, AB, Canada

Introduction

C-arms are mobile fluoroscopy machines that are an increasingly pervasive imaging modality in orthopedic surgeries. Evidence indicates that manual positioning of C-arms throughout surgery leads to excess time and radiation exposure [1, 2]. In addition, C-arms are primarily used qualitatively. The goal of this research is to develop a sufficiently accurate position measurement system for the C-arm base that is unobtrusive enough to use in an operating room.

Medical Radiation Technologists (MRTs) are normally responsibly for maneuvering C-arms during surgery based on verbal instructions from the surgeon. Trial-and-error X-rays, commonly called scout images, are often taken while positioning the C-arm to capture a specific radiographic view. These scout images increase operation time and lead to unnecessary excess radiation exposure for patients and staff [1].

The frequency of C-arm repositioning during surgery is dependent on the complexity of the procedure. One study reported an approximate range of 10–50 C-arm positional changes during orthopedic trauma cases [2]. In this study, moving the entire C-arm using the base wheels constituted a majority of the movements. Surgeons commonly require that several specific X-ray images be repeated multiple times to monitor the position of tools or implants. Scout images are typically necessary to achieve the requested previous position. Eighty percent of all C-arm motion during orthopedic trauma surgery is reportedly related to repeating a previous radiographic view [1, 2]. A tracked C-arm could provide positioning guidance to MRTs to reduce the need for scout images.

In addition to reducing radiation exposure, position tracking can be used to expand C-arm functionality. The size of the anatomic view in a single image can be increased by virtually stitching multiple C-arm images together to create an expanded panorama [3]. A tracked C-arm could also be used to provide navigation assistance. Studies have shown that computer-assisted navigation increases placement and alignment accuracy for implants [4–6].

To address these opportunities, various research groups have created tracking systems for C-arms. External optical tracking is a commercially available method for C-arm position tracking [7], but it is limited by the need to maintain line-of-sight, the obtrusiveness of the camera hardware, and by the high cost of commercial tracking systems. Electromagnetic tracking avoids the need for line-of-sight, but proposed solutions have limited range [8] and are prone to errors in the presence of metal objects [9]. Several tracking systems have been suggested that use optical patterns placed on or attached to the operating table to calculate the C-arm pose [9–11]. Limitations of these systems include the need to modify the operating table and limits on the tracking range. Some systems track the C-arm joints by using Inertial Measurement Units but presume that the base remains fixed [3]; such systems would be complementary to base-tracking capabilities.

To address these limitations of previous systems, we therefore propose and evaluate the performance of a less-obtrusive base-tracking system for C-arms called OPTIX (On-board Position Tracking for Intraoperative X-rays) that uses an on-board camera mounted beneath the C-arm base to measure motion using the visual texture present in operating room floors.

Tracking system requirements

The degree of accuracy required for the OPTIX system is determined by the clinical applications to be supported. One area of significant interest is in repositioning tasks, in which it is desired to retake a radiographic image from the same perspective as the original (e.g., in iliosacral screw insertion). In a recent study evaluating the performance of orthopedic surgeons, the position and rotation variabilities accepted by expert surgeons were up to 4.3 cm and 3.8°, respectively [12].

We further constrained the angular error by considering a repositioning task where an anatomical feature must be within the field of view of the C-arm. The imaging center of the C-arm is approximately 80 cm from the wheeled base so a rotational error at the base creates a lateral displacement at the imaging center. The rotational error must be less than $\tan^{-1}\left({}^{4.3}/_{80}\right) = 3.1°$ to ensure that the center point of the imaging is within the desired 4.3 cm for repositioning tasks,

Other base-tracking applications, such as generating stitched image panoramas or measuring limb lengths, require more stringent translation error bounds. Recent research has determined that errors on the order of 5 mm can be considered clinically acceptable for the purpose of intraoperatively evaluating scoliosis alignment using panoramic images [13]. The value of 5 mm was chosen to enable a measurement of the sagittal vertical axis misalignment within 10% of the value known to correlate with a higher quality of life [14]. Similarly, in surgeries in which limb lengths need to be equalized, limbs are considered acceptably equal if their lengths differ by less than 5 mm [15]. A base-tracking system with a 5 mm accuracy would therefore meet clinical needs.

The upper bounds for the tracking system were set as 5 mm for translational error and 3.1° of rotational error according to the needs of the chosen applications.

Methods

The proposed OPTIX system involves three principal design stages: (1) instrumenting the C-arm with camera hardware, (2) camera calibration, and (3) algorithm development. The system's tracking accuracy was then validated in a simulated operating room.

Hardware

The components of the tracking system include: a camera, a processor, a display for user interaction, a mounting system, and on-board lighting. The optimal camera location was first considered in order to design the necessary mounting hardware. The camera was required to be mounted in a position that would not be affected by the regular motion of personnel during surgical procedures. Behind the front wheels of C-arms from common manufacturers (e.g., Siemens, Munich, Germany; Philips, Amsterdam, Netherlands; General Electric, Boston, USA; Ziehm, Nuremberg, Germany) there is a hollow space that provides a sheltered mounting location. The downside of this location on the wheeled base is that the camera field of view is limited due to the close proximity to the floor. We therefore opted to use a camera (CM3-U3-13S2M-CS, FLIR Integrated Imaging Solutions Inc., Richmond, Canada) with a low (29 mm) vertical profile to maximize the distance between the camera and the floor. The technical specifications of the imaging system are detailed in Table 1.

An Odroid-XU4 board was chosen as the processing unit and an Odroid-VU7 + touch screen display was used as the interface. The Odroid system was chosen because it has a multi-core CPU that supports parallel processing and is small enough to fit within the limited available space. A ring of white LEDs in a custom-made holster surrounded the camera lens to provide illumination. Self-contained illumination is important to ensure consistent lighting conditions beneath the C-arm regardless of changing lighting in the surrounding environment. We designed a custom mounting platform to mount the camera and processing unit to the C-arm through two pre-existing holes in the front wheel strut, shown in Fig. 1. The wheel struts are at an angle to the floor, so the mounting platform has adjustable slots to enable the camera to be aligned perpendicular to the floor.

The system is created using mostly off-the-shelf components except for the mounting system, which was 3D printed. The total cost was approximately C$800, which is considerably lower than the tens of thousands of dollars associated with conventional tracking systems.

Algorithms

The operation of this system relies on two calibration algorithms and a base-tracking algorithm. The calibration procedures include: (1) an undistortion calibration to account for lens distortions, and (2) a scale calibration to determine the mapping of image coordinates to world coordinates. The base-tracking algorithm has two operating modes: (1) frame-to-frame relative tracking and (2) absolute position recovery.

Software packages

The calibration procedure and base-tracking algorithm programs were both written in Python 2.7, and several established algorithms were obtained from OpenCV 3.1, an open source library for computer vision, for calibration and tracking. The Odroid operated on Ubuntu 16.04.

Table 1 Technical details of the camera (1), and lens system (2)

Make and model	Imaging sensor	Imaging architecture	Resolution	Frame rate	Machine vision standard	Focal length
(1) FLIR CM3-U3-13S2M-CS	1/3″, 3.75 mm pixels	Global shutter CCD	1288 × 964	30 fps	USB3 vision v1.0	2.8–8 mm
(2) Fujinon YV2.8 × 2.8SA-2						

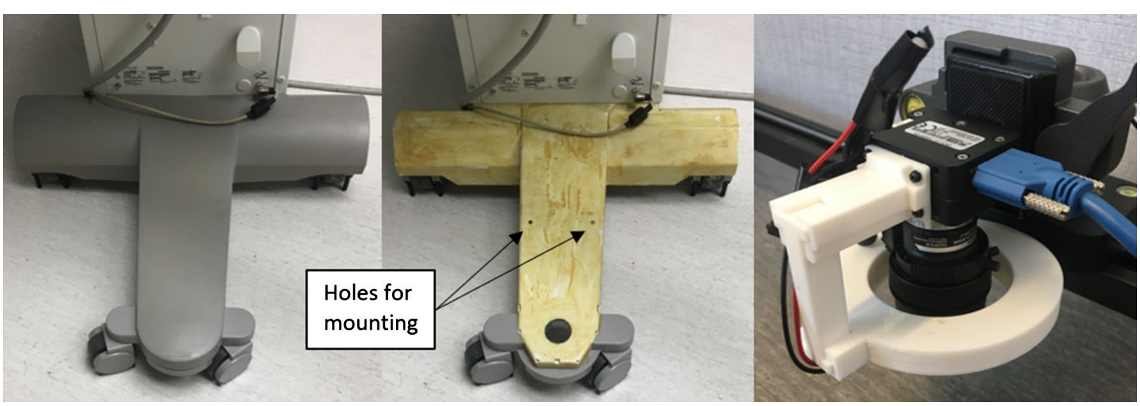

Fig. 1 (left) Wheeled base of the C-arm, (center) wheeled base after removing the rubber to reveal two holes available for mounting, (right) camera with attached light ring

Undistortion calibration

To correct lens distortions, we employed an established, closed-form calibration technique [16], which uses photos of a physical checkerboard pattern taken from multiple angles. This is a standard geometric camera calibration procedure that is built into OpenCV and is performed once for a given camera and lens setup.

Scale calibration

The scale calibration procedure uses a custom square target [17]. Digital calipers were used to measure the physical lengths of the sides of the square target, which were then used to calculate the scale value in units of millimeters per pixel. Figure 2 shows the calibration algorithm and a flowchart describing each step.

Relative motion tracking

The primary mode for the OPTIX system is frame-to-frame relative tracking. Feature points are detected in each image, as shown in Fig. 3 and the algorithm searches for matching features between subsequent images. The algorithm then calculates the incremental position and orientation change between each successive frame, and the C-arm pose is updated continuously in real-time.

The origin of the coordinate system for the tracking algorithm is taken to be the initial location of the C-arm. The axes are established relative to a user standing at the back of the C-arm; the y-axis extends away from the user toward the front of the C-arm and the x-axis is drawn horizontally to the right from the perspective of the user. Looking down at the C-arm from above, a counter-clockwise rotation is considered positive. The steps of the relative tracking algorithm are illustrated in Fig. 4.

A rigid transformation matrix is calculated for each set of consecutive video frames. The incremental rotation and translation are obtained from the rigid transformation matrices. These incremental changes are then used to update the cumulative rotation and displacement for the C-arm base. The rotation and displacement are contained in the rigid transformation matrix as follows:

$$\text{Rigid} = \begin{bmatrix} R_{1,1} & R_{1,2} & T_1 \\ R_{2,1} & R_{2,2} & T_2 \end{bmatrix} = \begin{bmatrix} \cos(\Delta\text{yaw}) & -\sin(\Delta\text{yaw}) & T_x \\ \sin(\Delta\text{yaw}) & \cos(\Delta\text{yaw}) & T_y \end{bmatrix}, \tag{1}$$

where Δyaw is the incremental 2D rotation between the current frame and the previous one. T_x and T_y are, respectively, the x and y displacements between the current frame and the preceding frame.

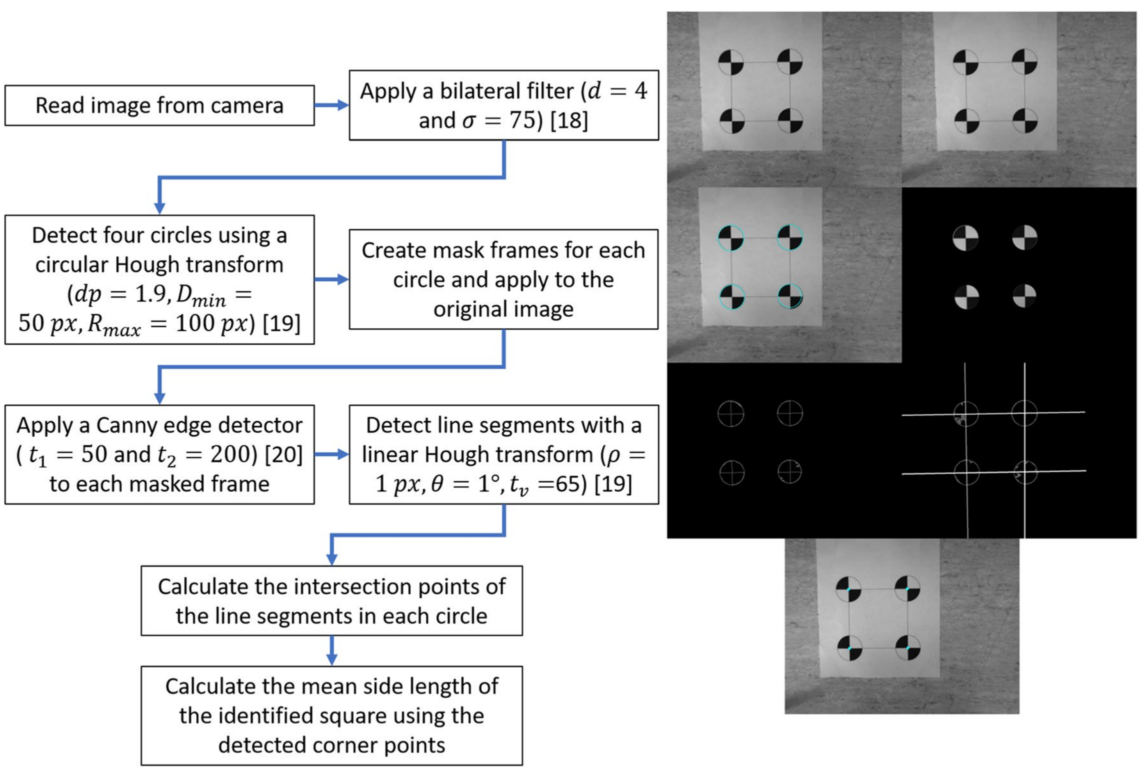

Fig. 2 Flowchart and images describing the scale calibration algorithm. The boxes on the left describe the corresponding images on the right [18–20]

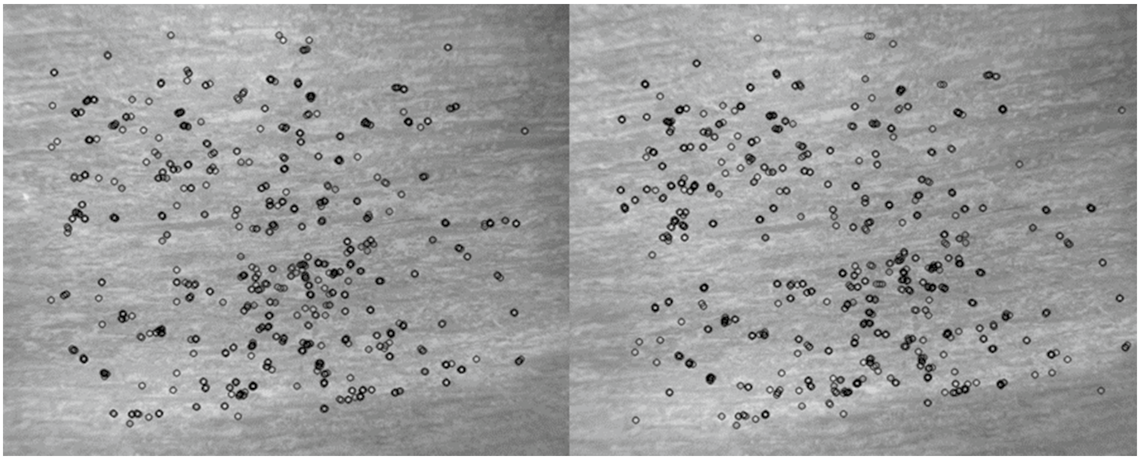

Fig. 3 Example images with ORB [21] features detected on the operating room floor. The two images were taken approximately 5 mm apart

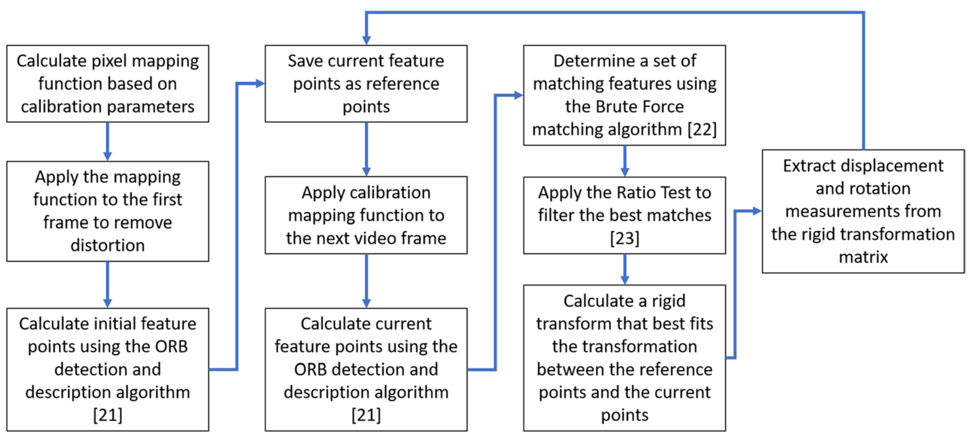

Fig. 4 Flowchart of the relative motion tracking sequence [21–23]

The following shows how the incremental rotation is calculated based on the rigid transformation matrix above:

$$\Delta\text{yaw} = \tan^{-1}\left({R_{2,1}}/{R_{1,1}}\right) = \tan^{-1}\left({\sin(\Delta\text{yaw})}/{\cos(\Delta\text{yaw})}\right). \tag{2}$$

The rotation component of the current C-arm location, θ, is calculated by summing up all the incremental yaw rotation measurements.

The incremental displacements between successive video frames are tilted relative to the initial coordinate axis by θ, and are measured in pixels. The scale factor, λ (mm/pixel), obtained from calibration, and the total rotation, θ, are therefore used to transform the incremental displacements to the global coordinate system:

$$\begin{bmatrix} \Delta X \\ \Delta Y \end{bmatrix} = \lambda \begin{bmatrix} \cos\theta & -\sin\theta \\ \sin\theta & \cos\theta \end{bmatrix} \begin{bmatrix} T_x \\ T_y \end{bmatrix}. \tag{3}$$

The total displacement in global coordinates, X and Y, is the summation of incremental changes, ΔX and ΔY. The C-arm base pose represented in global coordinates, (X, Y, θ), is updated in real-time by continuously accumulating incremental rotation and displacement values. At present, the algorithm for relative tracking achieves a processing speed of approximately 8 frames per second.

Absolute position recovery

We implemented an absolute position recovery mode that allows users to log the present C-arm position at any time and provides guidance in returning to a saved position, which is motivated by a clinical need to re-take multiple X-rays from previous positions. When a position of interest is selected by the user to be saved, the rotation and translation information is recorded in global coordinates, as well as the complete set of feature points and descriptors for the visible points. When the C-arm is maneuvered to a location that is sufficiently close to a selected saved position (defined as being within 3 cm, which ensures sufficient overlap of images to enable reliable matching of feature points), the system switches modes and calculates the current position relative to the saved position instead of using frame-to-frame tracking, thereby eliminating accumulated errors. When the C-arm moves sufficiently far away from a saved point, the relative tracking mode resumes.

Graphical user interface

We created a straightforward graphical user interface (GUI) to allow the user to interact with the tracking system. The GUI, shown in Fig. 5, has two main tabs: tracking and calibration. The calibration tab is only used during initial calibration, while the tracking tab is used to carry out the base-tracking functions. In the tracking mode (shown), the circles indicate saved points (with the clinically relevant tolerance bounds indicated in gray), while the C-arm position and orientation are indicated by the overlaid square with crosshairs to guide rotational alignment.

Verification and validation experiments

Linear track

A linear track experimental setup was created for initial algorithm development and used for initial accuracy testing. The camera was mounted on a 1 m linear sliding track and aimed at the floor. The track length was measured using a measuring tape and the camera was manually propelled back and forth until a cumulative distance of 2 m was reached. This measurement was compared to the results calculated by the tracking algorithm to provide a baseline for the algorithm performance before including the effects of mounting the camera on a C-arm and allowing multi-degree-of-freedom movements.

Simulated operating room

We evaluated the accuracy of the OPTIX system using a Siemens Arcadis Orbic Mobile C-arm (Siemens, Erlangen, Germany) located at our research Centre for Hip Health and Mobility. Real operating room conditions were recreated using our simulated surgical suite, shown in Fig. 6. The reference standard tracking system was an Optotrak Certus (Northern Digital Inc., Waterloo, ON, Canada) optical tracking system. The Optotrak measurements were compared with OPTIX measurements to calculate tracking errors. The manufacturer-stated resolution and error for the Optotrak are 0.01 mm and ± 0.1 mm, respectively [24].

Three infrared markers were taped to the main body of the C-arm with a separation of approximately 20 cm (see Fig. 7). The estimated angular error for this separation was calculated as $\tan^{-1}\left({}^{0.1\text{ mm}}/_{200\text{ mm}}\right) = 0.03°$, according to the stated Optotrak error rate.

Optotrak measurements are oriented in a local coordinate system for each infrared marker, while the OPTIX tracking system calculates the C-arm pose relative to the starting position. The motion calculated by OPTIX is assumed to be parallel to the floor plane. To compare the results from Optotrak and OPTIX, the Optotrak measurements were projected onto the floor plane and converted to rotation and translation relative to the C-arm starting position.

At the beginning of each test session we measured 6 locations on the floor with a probe (Northern Digital Inc., Waterloo, ON, Canada) to establish the floor plane, which is

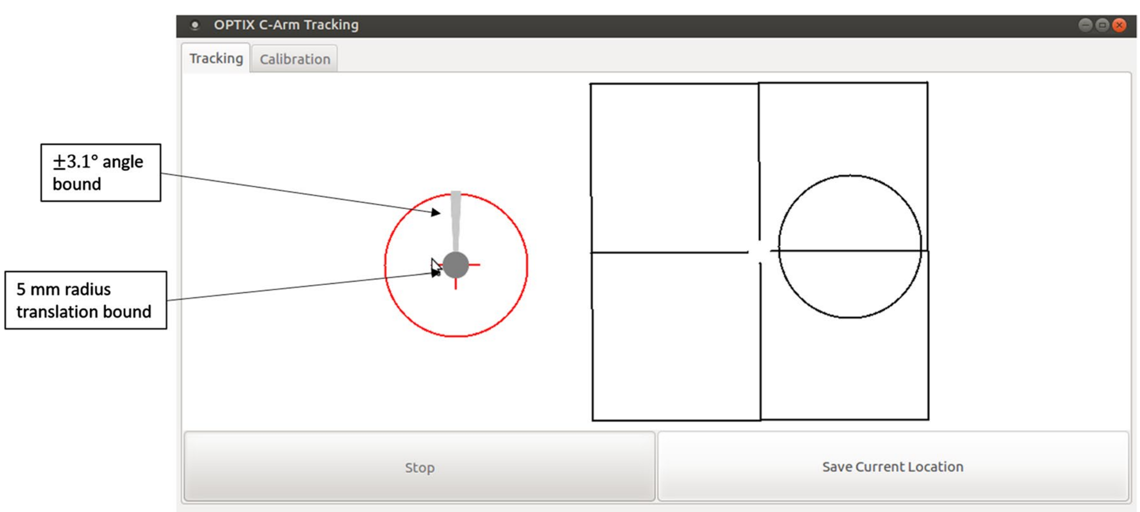

Fig. 5 GUI for OPTIX. Two saved points are shown as large circles. The red circle is currently selected while the black circle shows an unselected saved point. The labeled light gray triangle and dark gray filled circle, respectively, depict 3.1° and 5 mm bounds

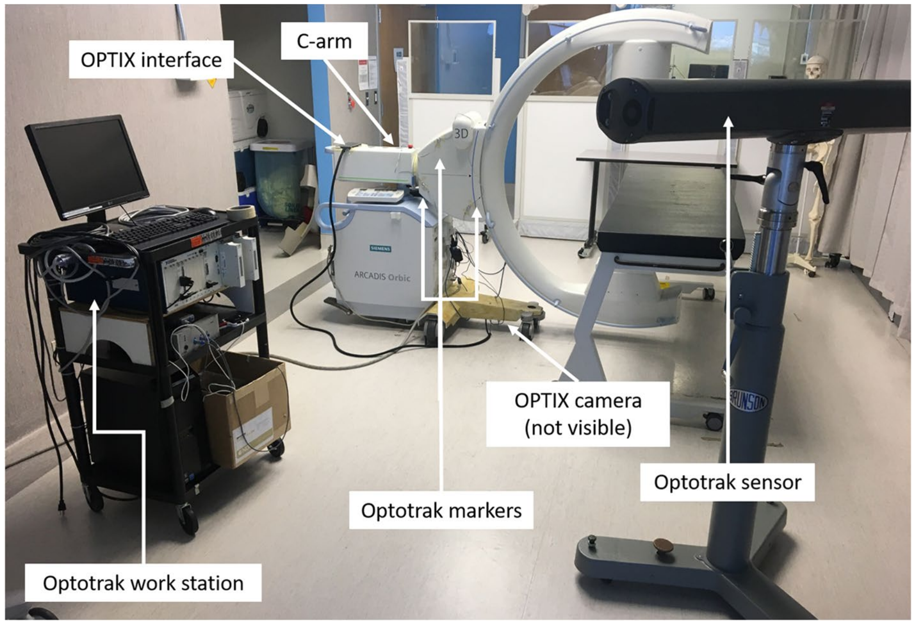

Fig. 6 Setup for C-arm testing

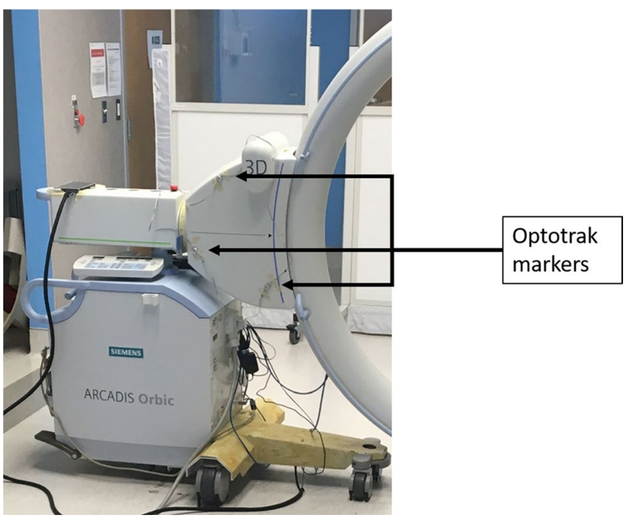

Fig. 7 Three infrared markers mounted to the C-arm for Optotrak tracking

assumed to be planar. All Optotrak measurements in a given test session were projected onto the measured floor plane to calculate C-arm motion. This process essentially constrained the measured motion to a single plane.

A point measured from an infrared marker, described in Optotrak coordinates as $P_{\mathrm{opt}} = \left[x_{\mathrm{opt}} \ y_{\mathrm{opt}} \ z_{\mathrm{opt}} \right]$, was projected onto the plane described by a normal vector $N_{\mathrm{floor}} = \left[u \ v \ w \right]$ and an arbitrary point on the plane $Q_{\mathrm{floor}} = \left[x_{\mathrm{floor}} \ y_{\mathrm{floor}} \ z_{\mathrm{floor}} \right]$ according to Eq. 4.

$$P_{\mathrm{proj}} = P_{\mathrm{opt}}\left(I_{3\times3} - N_{\mathrm{floor}}^{T} N_{\mathrm{floor}}\right) + Q_{\mathrm{floor}}\left(N_{\mathrm{floor}}^{T} N_{\mathrm{floor}}\right) \tag{4}$$

where P_{proj} is the calculated projected point and $I_{3\times3}$ is an identity matrix of size 3×3.

The infrared markers were rigidly mounted to the C-arm and the only motion that occurred during the experiments was due to the wheeled C-arm base, so the markers did not move relative to one another.

A local coordinate system was defined for each set of Optotrak measurements. The coordinate system was described by the vectors between the infrared markers, which were used to calculate a set of normalized orthogonal axes $(i, j, k)_n^m$, where m is the marker number and n is the coordinate frame. The initial orientation of the C-arm was defined using the axes of the local coordinate system calculated at the starting position.

The camera location, $\left(x_c, y_c, z_c\right)$, which was measured using the probe, was combined with the rotation matrix to fully establish the starting pose of the C-arm in global coordinates. The transformation matrix T_{G0}, which describes the relationship between the Optotrak coordinate system G and the local coordinate system O, is given by the following, based on [25].

$$T_{G0} = \begin{bmatrix} 1 & 0 & 0 & 0 \\ x_c & i_0^1 & j_0^1 & k_0^1 \\ y_c & i_0^2 & j_0^2 & k_0^2 \\ z_c & i_0^3 & j_0^3 & k_0^3 \end{bmatrix} \tag{5}$$

This initial pose is the origin point in the OPTIX system, so planar-constrained Optotrak position changes are calculated relative to this pose for direct comparison. At every C-arm position during a test session, transformation matrices, T_{Gi}, for the local coordinate system were calculated. The subsequent C-arm position, T_{0i}, was then determined in relation to the initial location T_{G0}:

$$T_{0i} = T_{G0}^{-1}\, T_{Gi} \tag{6}$$

The motion is assumed to be constrained to the floor plane, so the Z-axis was chosen to be normal to the floor for convenience. The global transformation matrices for any position relative to the initial position have the following form:

$$T_{0i} = \begin{bmatrix} 1 & 0 & 0 & 0 \\ x_i & \cos\theta_i & -\sin\theta_i & 0 \\ y_i & \sin\theta_i & \cos\theta_i & 0 \\ 0 & 0 & 0 & 1 \end{bmatrix}. \tag{7}$$

The translation and rotation information in this transformation matrix is in the same coordinate system as the OPTIX measurements. The C-arm displacement and orientation relative to the initial point were therefore extracted directly from each transformation matrix.

Verification of relative tracking algorithm accuracy

The relative tracking accuracy evaluations were separated into tests for translation and rotation. The goal for these tests was to evaluate the accumulation of tracking error with increasing distance or rotation. For translation testing, the C-arm was moved through a range of distances up to 3.5 m, approximately two times the length of a regular operating table. For rotation, the C-arm was rotated up to 70°. During observations of orthopedic procedures, the largest rotation we recorded was approximately 35° in a one direction. Therefore, the maximum two-way rotation that we expect is approximately 70°.

In both sets of tests, the C-arm was held still between movements for 10 s to create easily identifiable synchronization points when post-processing the Optotrak and OPTIX data. The initial point was calculated as the mean position during the stopped time, which defined the start of each movement. The Optotrak measurements, $(X, Y, \theta)_{\mathrm{optotrak}}$, and OPTIX measurements, $(X, Y, \theta)_{\mathrm{optix}}$, were directly compared to calculate the tracking error for all relative tracking tests.

Verification of absolute position recovery accuracy

The accuracy of the absolute position recovery algorithm was determined through a set of repositioning tasks consisting of four predefined patterns of motion, which were chosen based on regular C-arm motion observed in the operating room. These four patterns were as follows:

(1) *Side-to-side translation* straight line motion along the full length of the operating table to emulate movements often observed during lower limb or spine surgery.

(2) *In–out translation* motion perpendicular to the operating room table, which occurs during pelvis fixation and spinal surgeries to create more room for the surgeon to work between X-rays.

(3) *Oblique motion* combined translation and rotation to represent maneuvers we observed during lower limb and spinal surgeries.

(4) *Multi-point sequences of four points* to evaluate OPTIX's ability to handle multiple save points in one session.

In all cases, the C-arm was maneuvered until the GUI showed a green target, indicating that the C-arm was adequately repositioned. The Optotrak, $(X, Y, \theta)_{\mathrm{optotrak}}$, and OPTIX, $(X, Y, \theta)_{\mathrm{optix}}$, measurements of this final resting position were directly compared to calculate the error in the position recovery algorithm.

Validation study: reacquiring X-ray images from a saved location

To evaluate the ability of OPTIX to provide useful guidance to a user for repositioning tasks, one user (author LH) acquired an X-ray image of a screw located in a phantom pelvis model, recorded the position with the GUI, maneuvered the C-arm in each of the three directions described in the previous section and then used the OPTIX guidance screen to reacquire the original position. Upon reacquisition, a second X-ray image was taken and overlaid on the original for comparison. The translational and rotational discrepancies were then measured with digital calipers using the screw head as the landmark for evaluating translations and the screw axis for evaluating rotations.

Results

Linear track

The translation error for the relative tracking and absolute position recovery algorithms after traveling 2 m were 2.9 mm and 0.3 mm, respectively, as shown in Fig. 8. The errors are both well within the desired threshold of 5 mm.

Relative motion tracking error

The translation error is depicted in Fig. 9 in relation to the cumulative distance travelled (as measured by the NDI Optotrak system) for the relative motion testing. The error stays below the 5 mm threshold until the C-arm travels approximately 0.7 m and is largely bounded by 0.75% lines. The data tended to be biased toward positive errors.

The relative rotation error is shown in Fig. 10. The errors are negatively biased but remain within the desired threshold of 3.1° up to a cumulative rotation of approximately 70°. The error rate is largely contained within a 5% line.

Absolute position recovery error

Figure 11 presents the mean errors in translation and rotation using the absolute position recovery algorithm during all repositioning tasks. Both the translation and rotation errors are well below the threshold values of 5 mm and 3.1°, respectively.

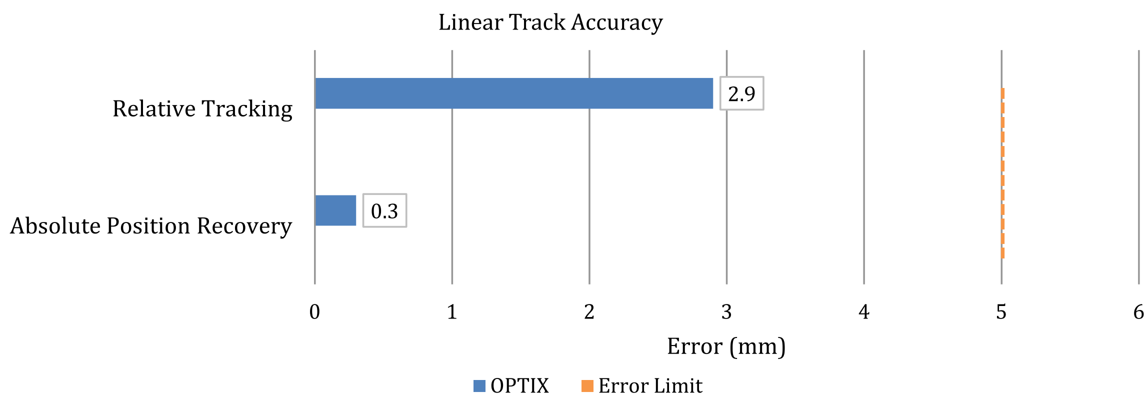

Fig. 8 Linear track errors for the relative tracking and absolute position recovery algorithms

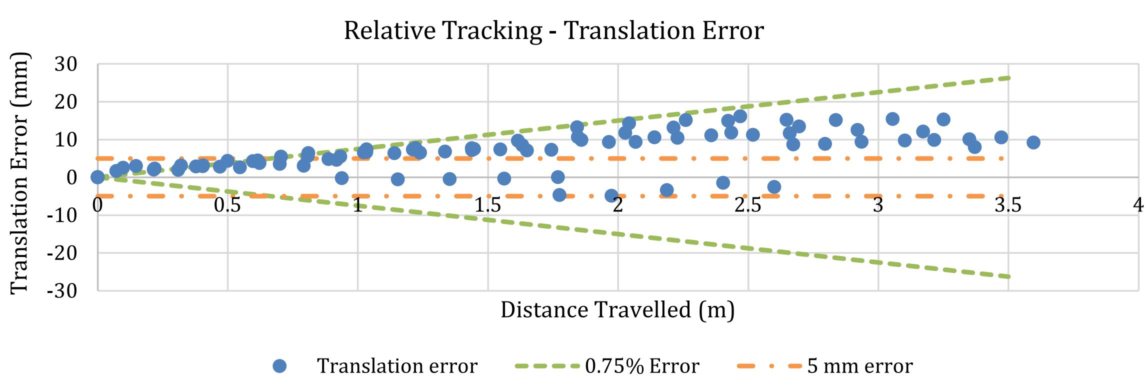

Fig. 9 Error in translation measurements for the relative tracking algorithm. The orange dash-dotted lines represent the 5 mm bounds for clinical acceptability, while the dashed green lines show that the error essentially remained within 0.75%

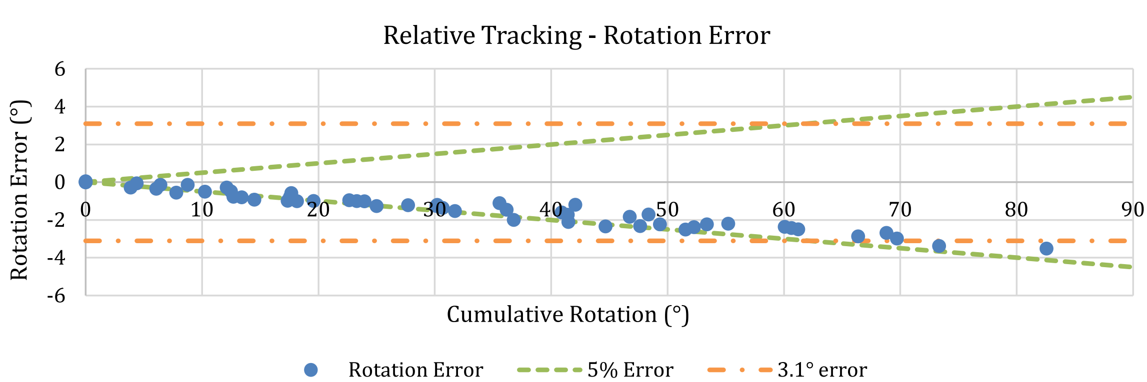

Fig. 10 Error in rotation measurements for the relative tracking algorithm. The orange dash-dotted lines depict the 3.1° error bounds for clinical acceptability, while the dashed green lines show that the error remained within approximately 5%

The translation error was also analyzed in relation to the cumulative distance travelled during repeated executions of the four repositioning motion patterns, as presented in Fig. 12. For every task and repetition the translation error remained with the ± 5 mm boundary. The standard deviation of the errors was only 1.5 mm, though several individual estimates had errors that were close to the 5 mm threshold.

The rotation error was also evaluated in relation to the cumulative distance, shown in Fig. 13. The rotation errors are all well below the 3.1° threshold lines and the standard deviation is 0.3°.

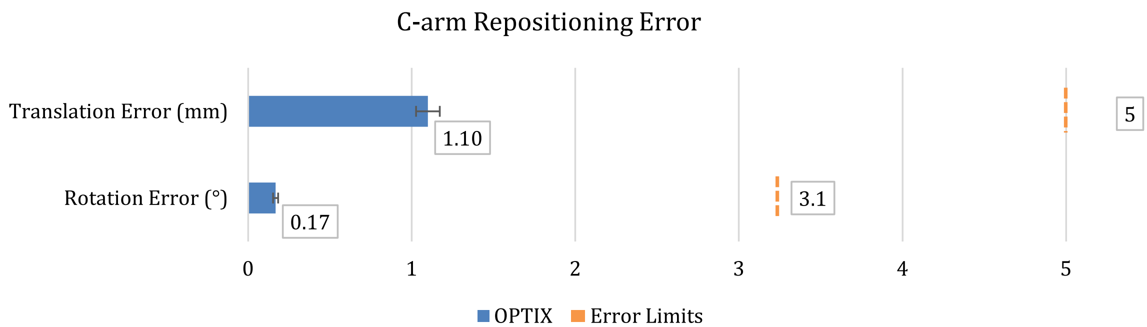

Fig. 11 Mean error for translation and rotation in repositioning tasks using the position recovery algorithm is shown in blue. The chosen accuracy thresholds are shown in orange

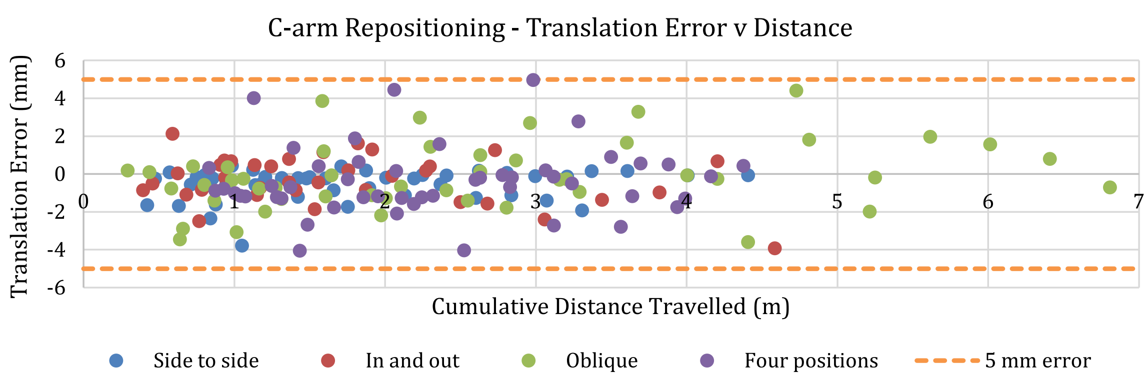

Fig. 12 Translation error in relation to distance travelled for all repositioning tasks using the position recovery algorithm. The dashed orange lines depict the desired error envelope

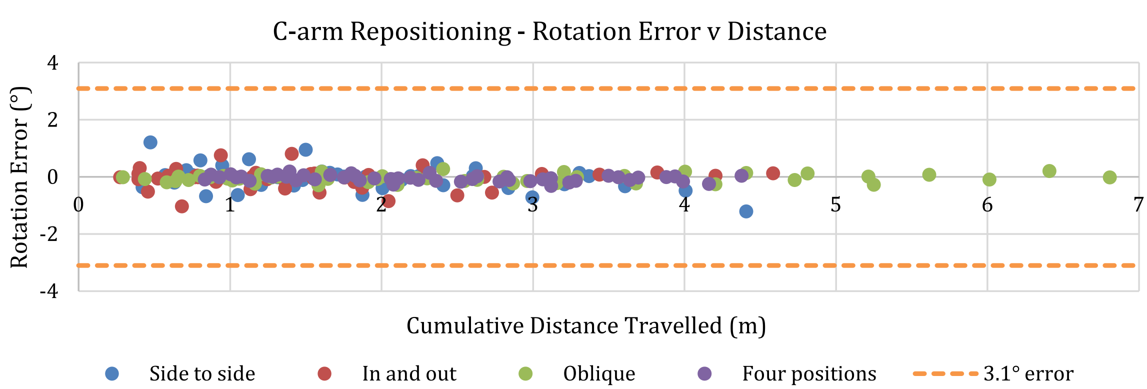

Fig. 13 Rotation error in relation to the distance travelled for all repositioning tasks using the position recovery algorithm. The dashed orange lines depict the desired error envelope

Reacquiring X-rays

Figure 14 shows the three reacquired X-ray images superimposed onto the initial X-ray with labeled translational and rotational differences. The translation was measured based on the left edge of each screw head, and the rotation was calculated using the centerlines. The desired outcome in this exercise was for the repeated images to be within 5 mm lateral distance and 3.1° of rotation from the initial X-ray. The labeled images show that the lateral errors were all within the desired tolerance and the rotational discrepancies were all well below the objective.

Discussion

This paper evaluated the ability of a downward-facing camera system to measure the movement of the base of a C-arm fluoroscopy machine using computer vision techniques. We found promising accuracy results in a simulated operating room setting for both relative tracking and absolute position recovery algorithms. The chosen error bounds for our experiments were driven by requirements for clinical applications, so these promising results motivate further development of this system.

This study builds on affiliated work [17], which provided the foundation for an offline monocular floor-facing camera and video odometry setup. The calibration procedure in this study was similar, but several notable improvements were implemented in the current system. We included an illumination system and upgraded the hardware to fit under the C-arm base as a self-contained unit. We developed a GUI for the operator to interact with the tracking algorithm and be presented with directional guidance. Finally, we made several significant changes to the tracking algorithms to enable real-time operation and incorporate an automatic absolute tracking mode.

Our system has demonstrated tracking accuracies that are comparable to or better than those reported by other research systems using more obtrusive tracking techniques. The resulting mean translation error of 1.10 ± 0.07 mm for all absolute position recovery tasks is comfortably within our defined requirement of 5 mm and is comparable to error rates reported by other research groups [8, 9]. However, our system achieves these accuracies without the need for modifying the operating table by installing special optical markers. The mean error in rotation we achieved for repositioning was $0.17 \pm 0.02°$, which is significantly lower than our defined acceptable error of 3.1°. The only other reported rotation error for a C-arm tracking system was four times larger than our result [9]. The OPTIX system is capable of tracking C-arm movements across distances approximately equivalent to those observed in clinical practice. This result is notable compared to several other systems in the literature that are limited in travel ranges [3, 10, 11].

We identified potential limitations to this novel research. A real operating room floor may have obstacles such as splattered blood that could influence the performance of our tracking system, although these could also potentially add useful features for the computer vision algorithm to use, if the field of view is not overly obscured. The system could have difficulty if an operating room is outfitted with flooring that is visually smooth with no trackable features, though we did observe that operating room floors in multiple hospitals all had similar flooring patterns [17]. In practice, a C-arm can be moved several meters away from the operating table during a procedure. While it would rarely be important to measure the position of the C-arm when removed from the table, the accuracy of its location would likely be within the 0.75% bounds for translation and 5% bounds for rotation error identified in our experiments. However, in principle,

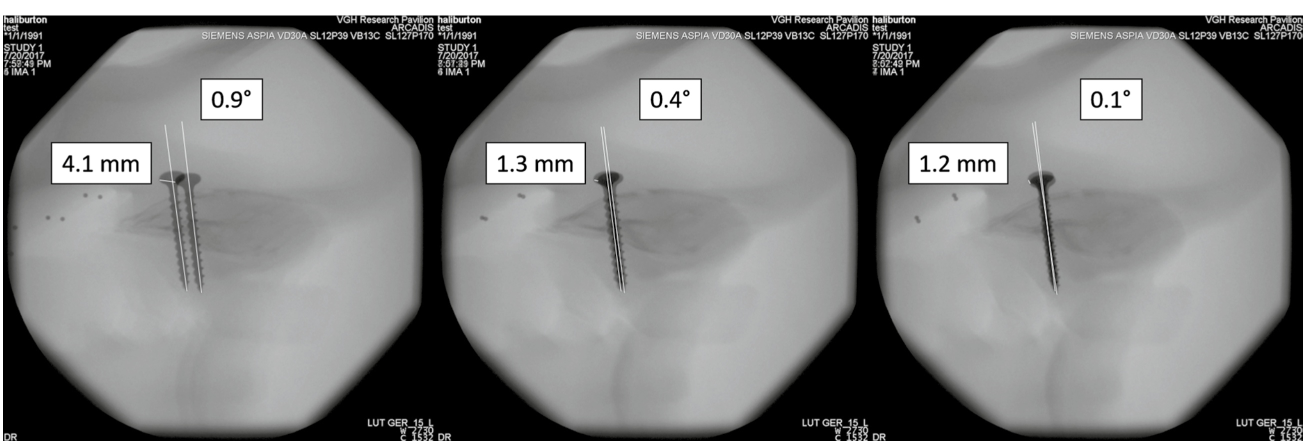

Fig. 14 Three repeated X-ray images superimposed onto the originals. The translation and rotation differences are labeled

the repositioning error after returning to the vicinity of the table should be within the 5 mm and 2° error bounds found in the repositioning tests. The magnitude of the rotation errors is likely linked to the size of the visible floor surface, which could potentially be considerably improved by adding a second camera at a distance from the primary camera to increase the effective "moment arm" of the rotation measurement. The error rates for the relative tracking algorithm tended to be positively biased for distance measurements and negatively biased for rotation. These biases could potentially be removed by adding a systematic correction algorithm to the system. Finally, all of our experimentation was conducted in a simulated operating room, so end-use environmental conditions may differ from the tested scenarios. For example, lighting conditions in a real operating room may not be the same as our simulated room, though we did use a standard operating room light in our studies. In addition, the shielded light source incorporated in the OPTIX tracking system is intended to limit the effect of changing external lighting conditions.

Conclusion

The OPTIX system has demonstrated that a tracking system using a single downward-facing camera can achieve clinically relevant tracking accuracy in a simulated operating room environment, and we conclude that the results justify further development aimed at deploying and evaluating the tracking system in a real operating room environment. The proposed OPTIX C-arm base-tracking system is accurate, unobtrusive, and low-cost. Importantly, the system avoids the issue of line-of-sight that hinders many conventional tracking systems. The tracking algorithms we created make use of several well-known techniques from computer vision, but the overall implementation and algorithm are novel developments, to the best of our knowledge.

The high localization accuracy and low-profile geometry of this system could likely allow it to be used as a generalized planar motion tracking system for other equipment whose motion on visually textured floors it would be valuable to track. Our system measures C-arm motion across the range of base movement expected in practice, including moving the C-arm away from the operating table, which has not been achieved in prior systems. The system has promising accuracy performance, and could be a step toward a highly useful system. Tracking the wheeled base of the C-arm on its own could contribute an accurate repositioning guidance system and reduce the need for scouting images. Further contributions could create a C-arm with accurate tracking for all degrees of freedom, leading to even more potential applications in the operating room. We believe that OPTIX has the potential to reduce excess operating time and exposure to radiation in the operating room for both patients and staff.

Acknowledgements The authors would like to thank the following for their support: Centre for Hip Health and Mobility (CHHM), Institute for Computing, Information, and Cognitive Systems (ICICS).

Funding This work was funded by the Natural Sciences and Engineering Research Council of Canada (NSERC) and by the Canadian Institutes of Health Research (CIHR) Collaborative Health Research Projects Program (Grant No. 462233-2014-CHRPJ).

Compliance with ethical standards

Conflict of interest The authors declare that they have no conflict of interest related to this work.

Ethical approval All procedures performed in studies involving human participants were in accordance with the ethical standards of the institutional and/or national research committee and with the 1964 Helsinki declaration and its later amendments or comparable ethical standards.

Human and animal rights This article does not contain any studies with animals performed by any of the authors.

Informed consent Informed consent was obtained from all individual participants included in the study. This article does not contain patient data. All evaluations were carried out by the authors.

References

1. Matthews F, Hoigne DJ, Weiser M, Wanner GA, Regazzoni P, Suhm N, Messmer P (2007) Navigating the fluoroscope's C-arm back into position: an accurate and practicable solution to cut radiation and optimize intraoperative workflow. J Orthop Trauma 21:687–692. https://doi.org/10.1097/BOT.0b013e318158fd42
2. Suhm N, Müller P, Bopp U, Messmer P, Regazzoni P (2004) The MEPUC concept adapts the C-arm fluoroscope to image-guided surgery. Injury 35:120–123. https://doi.org/10.1016/j.injury.2004.05.020
3. Amiri S, Wilson DR, Masri BA, Anglin C (2014) A low-cost tracked C-arm (TC-arm) upgrade system for versatile quantitative intraoperative imaging. Int J Comput Assist Radiol Surg 9:695–711. https://doi.org/10.1007/s11548-013-0957-9
4. Esfandiari H, Amiri S, Lichti DD, Anglin C (2014) A fast, accurate and easy to implement method for pose recognition of an intramedullary nail using a tracked C-arm. Int Arch Photogramm Remote Sens Spat Inf Sci XL-5:217–223. https://doi.org/10.5194/isprsarchives-XL-5-217-2014
5. Tian W, Zeng C, An Y, Wang C, Liu Y, Li J (2017) Accuracy and postoperative assessment of pedicle screw placement during scoliosis surgery with computer-assisted navigation: a meta-analysis. Int J Med Robot 13:e1732. https://doi.org/10.1002/rcs.1732
6. Todesca A, Garro L, Penna M, Bejui-Hugues J (2017) Conventional versus computer-navigated TKA: a prospective randomized study. Knee Surg Sports Traumatol Arthrosc 25:1778–1783. https://doi.org/10.1007/s00167-016-4196-9
7. Rudolph T, Ebert L, Kowal J (2010) Comparison of three optical tracking systems in a complex navigation scenario. Comput Aided Surg 15:104–109. https://doi.org/10.3109/10929088.2010.530793

8. Yoo J, Schafer S, Uneri A, Otake Y, Khanna AJ, Siewerdsen JH (2013) An electromagnetic “Tracker-in-Table” configuration for X-ray fluoroscopy and cone-beam CT-guided surgery. Int J Comput Assist Radiol Surg 8:1–13. https://doi.org/10.1007/s11548-012-0744-z
9. Moult, E, Burdette EC, Song DY, Abolmaesumi P, Fichtinger G, Fallavollita P (2011) Automatic C-arm pose estimation via 2D/3D hybrid registration of a radiographic fiducial. In: Medical imaging 2011: visualization, image-guided procedures, and modeling, vol 7964. SPIE, pp 839–846. https://doi.org/10.1117/12.877713
10. Reaungamornrat S, Otake Y, Uneri A, Schafer S, Stayman JW, Zbijewski W, Mirota DJ, Yoo J, Nithiananthan S, Khanna AJ (2011) Tracker-on-C: a novel tracker configuration for image-guided therapy using a mobile C-arm. Comput Assist Radiol Surg Berl Ger 22–25
11. Wang L, Traub J, Heining SM, Benhimane S, Euler E, Graumann R, Navab N (2008) Long bone X-ray image stitching using camera augmented mobile C-arm. In: Metaxas D, Axel L, Fichtinger G, Székely G (eds) Medical image computing and computer-assisted intervention—MICCAI 2008. Springer, Berlin, pp 578–586
12. Touchette M (2017) Artificial X-ray imaging system (AXIS)—design and evaluation on c-arm performance in operating room and educational settings. (Masters thesis). University of British Columbia
13. Amini M (2016) A fluoroscopy-based intraoperative tool for measuring alignments in spinal deformity correction surgery (Masters thesis). University of British Columbia
14. Schwab F, Patel A, Ungar B, Farcy J-P, Lafage V (2010) Adult spinal deformity—postoperative standing imbalance: how much can you tolerate? An overview of key parameters in assessing alignment and planning corrective surgery. Spine 35:2224–2231. https://doi.org/10.1097/BRS.0b013e3181ee6bd4
15. Clavé A, Sauleau V, Cheval D, Williams T, Lefèvre C, Stindel E (2015) Can computer-assisted surgery help restore leg length and offset during THA? A continuous series of 321 cases. Orthop Traumatol Surg Res 101:791–795. https://doi.org/10.1016/j.otsr.2015.08.003
16. Zhang Z (2000) A flexible new technique for camera calibration. IEEE Trans Pattern Anal Mach Intell 22:1330–1334. https://doi.org/10.1109/34.888718
17. Esfandiari H, Lichti D, Anglin C (2017) Single-camera visual odometry to track a surgical X-ray C-arm base. Proc Inst Mech Eng [H] 231:1140–1151. https://doi.org/10.1177/0954411917735556
18. Tomasi C, Manduchi R (1998) Bilateral filtering for gray and color images. In: Sixth international conference on computer vision (IEEE Cat. No. 98CH36271). Narosa Publishing House, Bombay, India, pp 839–846
19. Hough PV (1962) Method and means for recognizing complex patterns. US3069654A
20. Canny J (1986) A computational approach to edge detection. IEEE Trans Pattern Anal Mach Intell PAMI 8:679–698. https://doi.org/10.1109/TPAMI.1986.4767851
21. Rublee E, Rabaud V, Konolige K, Bradski G (2011) ORB: an efficient alternative to SIFT or SURF. In: 2011 international conference on computer vision, pp 2564–2571
22. OpenCV Dev Team OpenCV documentation: feature. (Accessed 03 Nov 2019)
23. Lowe DG (2004) Distinctive image features from scale-invariant keypoints. Int J Comput Vis 60:91–110. https://doi.org/10.1023/B:VISI.0000029664.99615.94
24. Northern Digital Inc (2015) Optotrak Certus: technical specifications
25. Zatsiorsky VM (1998) Kinematics of human motion. Human Kinetics, Windsor